SUPPLEMENTAL INFORMATION

SUPPLEMENTARY FIGURES DR1-4

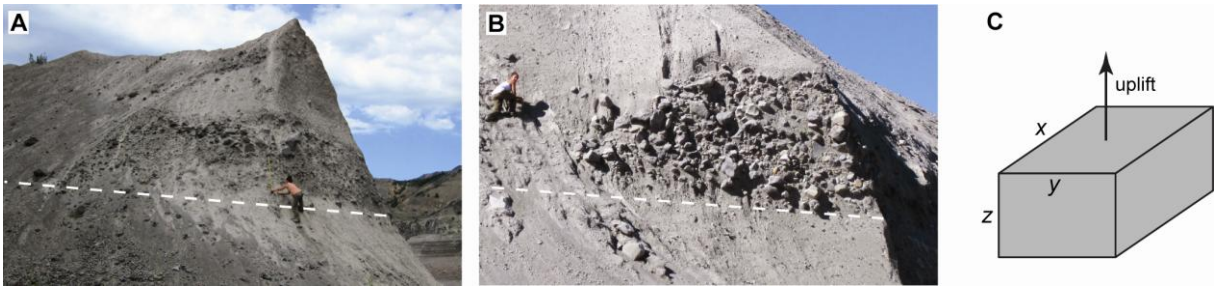

Figure DR1. Blocks entrained by pyroclastic flows at Mount St Helens. (A) Site 1 and (B) site 2 of Fig. 1 (persons for scale). Coordinates WGS84, UTM Zone 10 ; site 1: 560774 E, 5123399 N ; site 2: 561912 E, 5121594 N. The dashed line indicates the approximate contact with underlying units. (C) Idealized parallelepiped shape of the blocks with sides of length *x*>*y*>*z*, with assumed direction of uplift (arrow). Side *y* is commonly not measurable because blocks are imbricated in the matrix of the pyroclastic flow deposits.

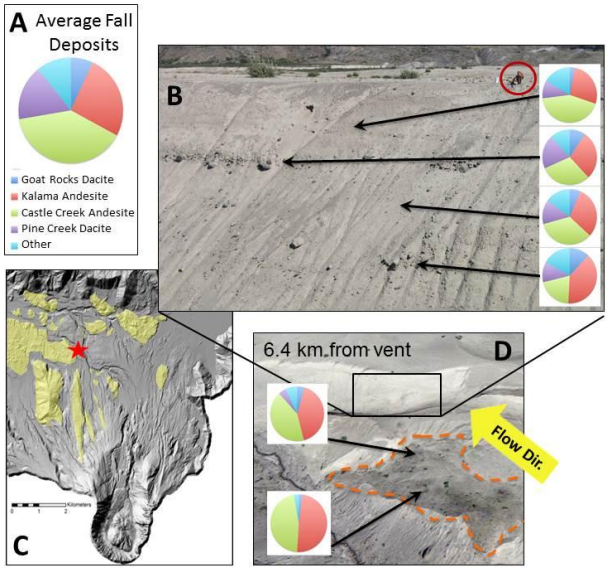

Figure DR2. Componentry of blocks in deposits at Mount St Helens. (A) Average componentry of the fall deposits. (B) Progressive depletion in the Kalama Andesite (red) indicates progressively less material was entrained from the debris avalanche deposit upstream from the outcrop (note person for scale). (C) Map of Mount St Helens and the pumice plain with red star indicating outcrop location. (D) Aerial view of the outcrop indicating the componentry of the debris avalanche deposit and inferred flow direction of the pyroclastic flow. The exposure in (B) is drawn in the box. Coordinates WGS84, UTM Zone 10 ; outcrop pictured in B: 560831 E, 5122392 N ; hummock pictured in D and outlined in orange: 560801 E, 5122290 N.

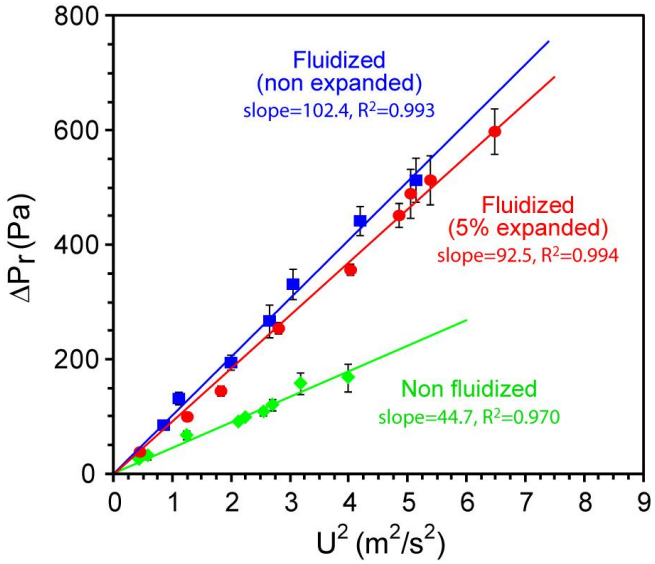

Figure DR3. Fits of data in Fig. 4A. Maximum relative underpressure on a rigid substrate, ΔP_r, as a function of the square of the flow front velocity, U^2, for initially fluidized and slightly expanded (~4-5%, ρ~1380 kg m^{-3}) or non-expanded (ρ~1450 kg m^{-3}) flows, and for non-fluidized flows (ρ~1450 kg m^{-3}).

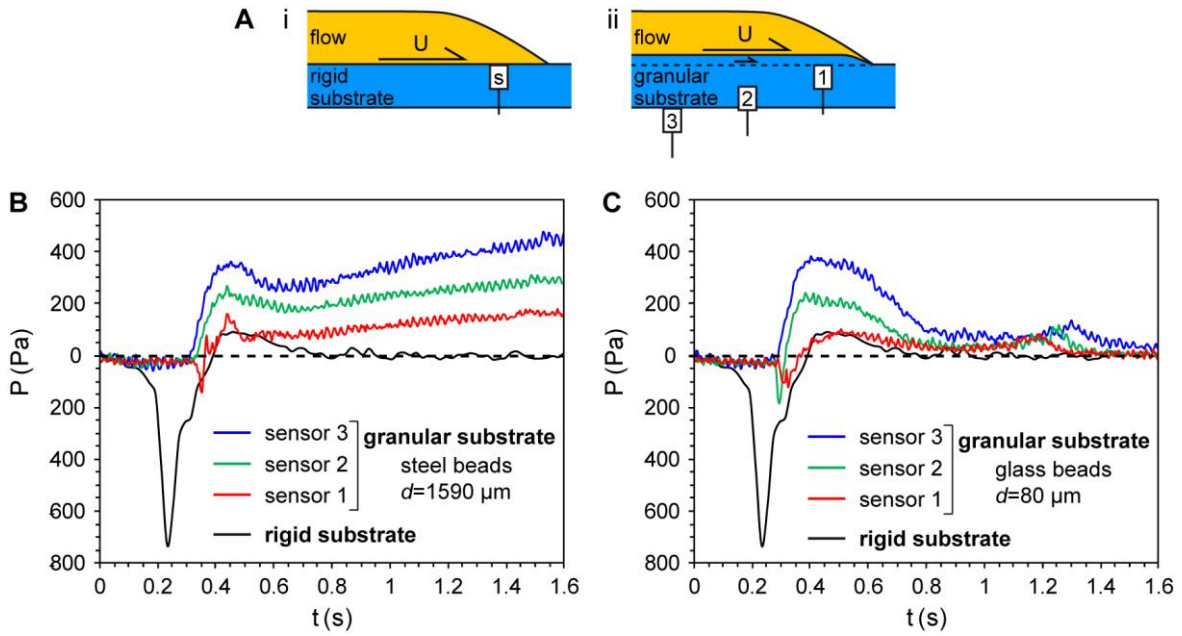

Figure DR4. Pore pressure generated by initially fluidized flows on rigid or granular substrates. (A) Sketches of flow of velocity U on (i) a rigid or (ii) a granular substrate (not to scale). In (i), a sensor (s) located at travel distance x=80 cm measures pore pressure at the top of the rigid substrate. In (ii), sensors are at depth h_s=3 cm (sensor 3, x=60 cm), h_s=1.5 cm (sensor 2, x=70 cm), and h_s=0 cm (sensor 1, x=80 cm, as in i), beneath the original top of the granular substrate. Entrainment of the substrate by the flow, at a low velocity ($<<U$, small arrow), displaces the flow-substrate interface upward, by a small amount equivalent to the height of the wavelike instabilities for a substrate of fines and to about one bead diameter for

a substrate of coarse particles. (B) Pressure measurements for a substrate of coarse steel beads (d=1590 µm) and flow velocity U=2.78 m s^{-1}. (C) Pressure measurements for a substrate of fine glass beads (d=80 µm) and flow velocity U=2.68 m s^{-1}. For comparison, the signal measured for a rigid substrate (case a-i, flow velocity U=2.70 m s^{-1}) is also shown. Time t=0 s corresponds to arrival of the flow front at the upper sensor at x=80 cm. For a granular substrate, and compared to a rigid substrate, upward displacement of the flow-substrate interface inhibits the generation of high underpressure, though a small peak of ~-100 to -150 Pa may be transiently generated at onset of flow deposition (t~0.3 s). The amount of overpressure generated by the flow body, however, is about of the same amplitude at the same travel distance (x=80 cm), while maximum overpressure at shorter travel distances (x=60 and 70 cm) is higher because the flow is less defluidized. Increase of pore pressure at late stages in case of a substrate of coarse beads (b) is due to percolation of the fine particles of the flow into substrate pore space.

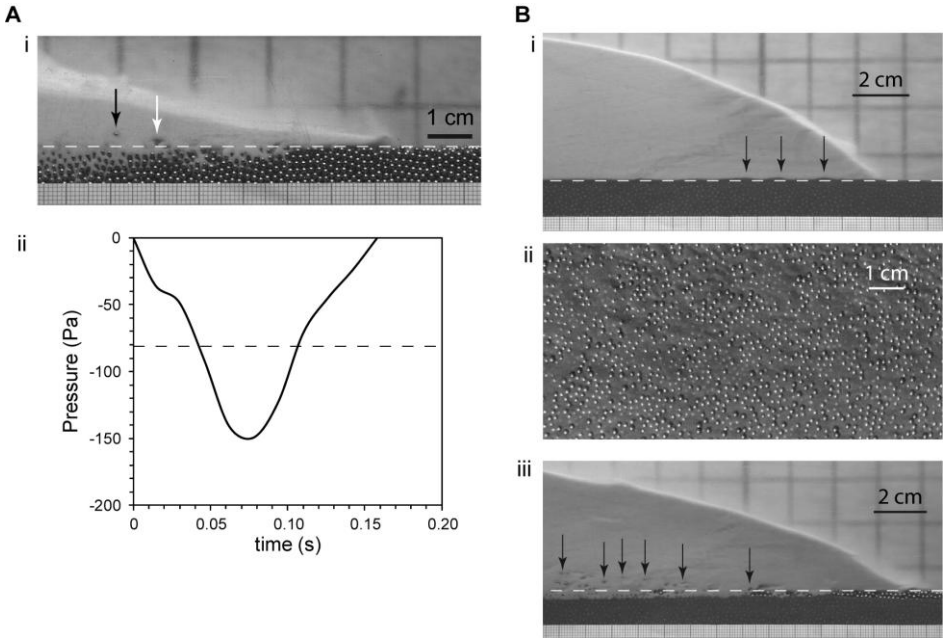

Figure DR5. Complementary experiments. (A) (i) First evidence of uplift (>1 mm, black arrow) from a rough substrate of steel beads (d=1590 µm) caused by an initially fluidized flow (U=1.30 m s^{-1}), ~0.045-0.050 s after passage of the front. The white arrow indicates an air bubble. (ii) Pressure generated by the sliding head of a similar flow (U=1.36 m s^{-1}) on a rigid substrate. The dashed line represents the critical underpressure for uplift (~–82 Pa, calculated from Equation 4), attained ~0.040 s after the flow front has passed the sensor (at 0 s). (B) Initially fluidized flows on substrates of binary mixture of coarse steel and fine glass beads (black). (i and ii) The black fines (d=80 µm) fill the network of coarse beads (d=1590 µm) up to its height; i: side view showing small shear wavelike instabilities (arrows), U=2.67 m s^{-1} (see Movie DR4); ii: top view of the substrate. (iii) The fines fill the network of coarse particles only up to ~1-2 bead diameter from the top. Percolation of fine flow particles (white) is limited and coarse beads are entrained individually (arrows), U=2.85 m s^{-1} (see Movie DR5).

SUPPLEMENTARY TABLES DR1-3

Supplementary Table DR1. List of experiments whose results are presented in Figure 4.

Rigid substrate			**Granular substrate** **Steel beads (d=1590 µm)**				**Granular substrate** **Glass beads (d=1600 µm)**			
n° Exp.	***U* (m/s)**	**ΔP_r (Pa)**	**n° Exp.**	***U* (m/s)**	**ΔP (Pa)**	***h* (mm)**	**n° Exp.**	***U* (m/s)**	**ΔP (Pa)**	***h* (mm)**
Non fluidized flow			*Non fluidized flow*				*Non fluidized flow*			
R1	0.67	26	G1	0.85	27	0.35	G38	0.55	11	0
R2	0.77	32	G2	1.38	71	0.9	G39	0.50	9	0
R3	1.12	68	G3	1.97	145	3.7	G40	0.57	12	0.3
R4	1.46	91	G4	1.89	134	3.9	G41	0.65	16	0.2
R5	1.60	109	G5	2.29	197	4.5	G42	0.71	19	0.45
R6	1.50	99	G6	0.52	10	0	G43	0.83	26	0.85
R7	1.65	121	G7	0.87	28	0	G44	0.95	34	1.1
R8	2.00	169	G8	1.08	43	0.4	G45	0.77	22	0.55
R9	1.78	158	G9	0.93	32	0.3	G46	0.63	15	0
Fluidized flow (non expanded)			G10	1.34	67	0.55	G47	0.75	21	0.5
R10	0.93	85	G11	1.46	80	1.6	G48	1.14	49	1.8
R11	1.06	131	G12	1.70	108	2.2	G49	1.41	75	2.8
R12	1.42	194	G13	1.68	106	2.5	G50	1.82	124	3.2
R13	1.75	331	G14	1.53	88	1.3	G51	2.25	190	3.7
R14	1.63	267	G15	0.73	20	0	G52	2.17	177	3.2
R15	2.05	442	*Fluidized flow (expanded)*				*Fluidized flow (expanded)*			
R16	2.27	512	G16	0.86	57	0.6	G53	0.37	11	0
Fluidized flow (expanded)			G17	1.04	84	0.6	G54	0.54	23	0.3
R17	0.68	38	G18	1.12	97	2.2	G55	0.48	18	0.3
R18	1.13	99	G19	0.95	70	0.2	G56	0.55	23	0.2
R19	1.36	144	G20	1.00	78	0.9	G57	0.43	14	0.35
R20	1.68	254	G21	1.23	117	2	G58	0.51	20	0.2
R21	2.01	356	G22	1.30	131	2.8	G59	0.63	31	1.3
R22	2.21	451	G23	1.29	129	3.6	G60	0.71	39	1.5
R23	2.25	489	G24	1.63	206	4.8	G61	0.92	66	1.8
R24	2.32	513	G25	3.06	727	7.3	G62	0.90	63	2.4
R25	2.55	598	G26	2.47	473	6.1	G63	2.11	345	4.5
			G27	2.55	505	6.6	G64	2.83	621	5
			G28	2.36	432	5.4	G65	3.2	795	5.8
			G29	1.97	301	5.3	G66	2.65	545	4.5
			G30	0.77	46	0.35	G67	2.44	462	4.9
			G31	0.57	25	0	G68	1.31	133	3.4
			G32	0.69	37	0.25	G69	1.15	103	2.7
			G33	0.47	17	0	G70	1.91	283	3.9
			G34	0.82	52	0.15	G71	0.57	25	0.65
			G35	1.46	165	3.3	G72	0.46	16	0.5
			G36	0.89	61	0.41	G73	0.41	13	0
			G37	1.10	94	1.45	G74	1.62	204	4
							G75	2.37	436	4.4
							G76	0.38	11	0
							G77	0.52	21	0.5
							G78	0.81	51	1.9
							G79	0.67	35	1.15

U: flow front velocity, ΔP_r: underpressure on a rigid substrate (Eq. 1), ΔP: pressure difference on a granular substrate (Eq. 3), *h*: maximum height of uplift of substrate beads (*h*=0 means beads dragged on the substrate).

Supplementary Table DR2. Complementary experiments.

n° Exp.	U (m/s)	Flow condition	Substrate	Figure
F1	0.85	non-fluidized	glass beads (d=80 µm)	
F2	1.37	non-fluidized	glass beads (d=80 µm)	
F3	0.93	fluidized	glass beads (d=80 µm)	
F4	1.46	fluidized	glass beads (d=80 µm)	3
F5	2.60	fluidized	glass beads (d=80 µm)	3
Pore pressure measurements				
P1	2.86	fluidized	steel beads (d=1590 µm)	
P2	2.87	fluidized	steel beads (d=1590 µm)	
P4	2.78	fluidized	steel beads (d=1590 µm)	DR4
P3	2.52	fluidized	glass beads (d=80 µm)	
P5	2.68	fluidized	glass beads (d=80 µm)	DR4
Substrates of binary mixture				
M1	2.67	fluidized	steel (d=1590 µm) + glass (d=80 µm) beads	DR5
M2	2.85	fluidized	steel (d=1590 µm) + glass (d=80 µm) beads	DR5

Supplementary Table DR3. Size of the five largest blocks entrained by pyroclastic flows at Mount St Helens.

Site	Coordinates WGS84, UTM Zone 10	Distance (km), slope (degree)	Longest x shortest axis (*x* x *z*, cm)* n° 1	n° 2	n° 3	n° 4	n° 5	Mean
1	560774 E, 5123399 N	5.6 km, <6°	55x47	43x36	68x24	49x35	50x33	53x35
2	561912 E, 5121594 N	7.2 km, <4°	92x31	30x30	32x30	37x24	32x12	45x25

* Middle axis *y* is commonly not measurable because of imbrication of the blocks in the ash matrix of the pyroclastic flow deposits.

EXPLANATION OF METHODS

Experiments

A column of glass beads of diameter of 80 µm was released by a lock-exchange system from a reservoir (Fig. 2). This generated a granular flow that propagated into a horizontal channel and eventually formed a deposit. The particles had a sub-horizontal trajectory, so that the flow was "laminar" by reference to single-phase fluid flows, and their velocity increased upwards (Roche et al., 2010; Girolami et al., 2010). Fluidized flows were generated by releasing a granular column at the base of which a vertical air flux was injected through a porous plate. The air flow velocity (U_{air}) was that required to generate drag enough to counterbalance the weight of the particles, which promoted interstitial pore fluid pressure proportional to the column height. The fluidized granular column was then non-expanded (at U_{air}=0.8 cm s^{-1}) or slightly expanded (~4-5%, at U_{air}=1.3 cm s^{-1}). The air-particle flow then defluidized progressively during propagation through slow pore pressure diffusion thanks to the low material permeability k~10^{-11} m^2 (Roche et al., 2010; Roche, 2012). Properties of the granular material adequately fulfilled scaling requirements regarding the natural system (Roche, 2012).

The channel substrate was either a rigid, smooth Perspex plate or consisted of a 3 cm-thick flat layer of spherical glass (d=80 µm or 1500 µm, ρ_p=2500 kg/m^3) or steel (d=1590 µm, ρ_p=7850 kg/m^3) beads. The granular layer was built by first pouring the beads, which were then levelled by means a vertical plate translated horizontally along the channel. Pore fluid pressure was measured at the top of the substrate by using piezoresistive sensors having a frequency response of 1 kHz (Roche et al., 2010). The sensors were covered by metallic grids of 38-µm aperture, which allowed transmission of the pore pressure and avoided impacts of granular flow particles. The experiments were filmed with a high-speed video camera at rates of 500-1000 frame/s. Images were processed to determine the mean initial top surface of the granular substrate and to track the motion of the substrate particles.

Field work

Mount St Helens

The May 18, 1980 eruption of Mount St Helens was initiated by collapse of the over-steepened north flank of the volcano (Criswell, 1987). The resulting landslide formed a debris avalanche deposit (DAD) throughout the pumice plain (area north of the volcano) over which later pyroclastic flows (PFs) propagated. The most voluminous and widespread PF deposits are characteristically massive and rich in lithic blocks. PF deposits directly downstream from DAD outcrops contain a higher percentage of coarse, dense, and often hydrothermally altered blocks. These blocks are outsized relative to blocks in PF deposits upstream from the DAD or where the DAD is absent, and as such are interpreted to have been derived (eroded) from a local source.

To identify locations where substrate erosion occurred, the componentry of lithics (i.e., of external origin) at various locations throughout the pumice plain, including PF, debris avalanche, and fall deposits, was compared. At each sample location more than 100 lithics, each >64 mm in diameter, were pulled from the deposit and classified into one of 21 lithologic categories based on mineralogy, grain size and texture (Fig. DR2). These 21 categories were placed into one of the four most recent eruptive periods from Mount St Helens: Pine Creek, Castle Creek, Kalama, and Goat Rocks (Mullineaux and Crandell, 1981). The fall deposits contain lithics entrained via conduit erosion. The componentry of the deposits of PFs with no evidence of interaction with the DAD is similar to the fall deposits, indicating that while some erosion possibly occurred on the steep flanks of the volcano, most lithics were derived due to vent erosion. The DAD tends to be dominantly mono- or bi-lithologic. An increase of the DAD components in downstream PF deposits relative to the fall and upstream PF deposits allowed us to identify blocks that were plucked, entrained and transported 10's of meters downstream. PF deposits downstream from DAD outcrops frequently have an increase of up to 50% of the rock type(s) that composed the DAD. The entrained lithic blocks are identified throughout the entire thickness of the two most voluminous 5-8 m-thick flow units produced during the climactic phase, but are often concentrated at the lower boundary.

Peach Springs Tuff

The outcrop of Peach Springs Tuff (PST) shown in Fig. 1C is located at N35°25′37.2″, W113°39′50.8″ near the town of Valentine, Arizona (USA). The location is ~80 km northeast of the PST's inferred source, the Silver Creek Caldera (Ferguson et al., 2013). The PST is a widespread silicic ignimbrite with variable degrees of welding, and its age is ~18.8 Ma (Ferguson et al., 2013).

In the area of interest (Fig. 1C), the ignimbrite was emplaced onto a surface with relatively low relief consisting of rolling hills of older granitic rocks and basaltic lavas. The

PST ponded and is mostly preserved where it deposited in topographic lows that locally formed a substrate of fluvial deposits with granitic and basaltic clasts (cobbles and boulders), such as the case illustrated here where the ignimbrite ranges from 10-15 m thick. The PST is massive and poorly sorted, with coarse-tail reverse grading of lithic clasts in its basal ~0.5 m, with normal grading of lithics and reverse grading of pumice clasts above that level. The basaltic clasts (blocks) shown in Fig. 1C differ from clasts found nearer to the source caldera, which are typically andesitic in composition. These basaltic clasts are locally derived, probably within a few hundred meters of the exposure. Other exposures in the PST-capped mesas around the town of Valentine contain similar locally derived basaltic clasts.

Criswell, C.W., 1987, Chronology and pyroclastic stratigraphy of the May 18, 1980 eruption of Mount St. Helens, Washington: Journal of Geophysical Research, v. 92, p. 237-266.

Mullineaux, D.R., and Crandell, D.R., 1981, The eruptive history of Mount St. Helens: U.S.G.S. Professional Paper 1250, p. 3-15.

Ferguson, C.A., McIntosh, W.C., and Miller, C.F., 2013, Silver Creek caldera - The tectonically dismembered source of the Peach Springs Tuff: Geology, v. 41, p. 3-6.

FLUIDIZATION OF A SUBSTRATE OF FINES

Substrate interstitial air can flow upward due to the pressure difference between the flow base and the substrate (ΔP). Considering Darcy's law and assuming that the typical length scales with the particle diameter, d, then the air flow velocity is

$$U_{af} \approx \frac{k}{\mu}\frac{\Delta P}{d}, \qquad \text{(DR1)}$$

where μ is the air dynamic viscosity (1.8×10^{-5} Pa.s) and k is the substrate permeability (~10^{-11} m^2 and ~10^{-9} m^2 for the fine and coarse beads, respectively). Comparing U_{af} with the minimum fluidization velocity, U_{mf} (~7×10^{-3} m s^{-1} for fine glass beads, ~2.6 m s^{-1} and ~9.2 m s^{-1} for coarse glass and steel beads, respectively), shows that a substrate of coarse beads cannot be fluidized (i.e., $U_{af}<U_{mf}$) in our experiments at ΔP up to ~700-800 Pa; in contrast, a substrate of fine glass beads can be readily fluidized (i.e., $U_{af}>U_{mf}$) even at the lowest pressure differences investigated (ΔP>30 Pa), so that individual particle uplift according to equation 4 is not efficient.

The wavelike instabilities at top of substrates of fines resemble bedforms generated by turbulent single-phase fluid flows, but the physical processes are of different nature. According to Rowley et al. (2011) and following the analysis of Farin et al. (2013), the granular flow and the underlying substrate can be considered as two fluids of different velocities and densities so that wavelike instabilities of Kelvin-Helmholtz type can arise if

$$U_1 - U_2 \geq \sqrt{\frac{g\gamma}{2\pi}\left(\frac{\varepsilon_2}{\varepsilon_1} - \frac{\varepsilon_1}{\varepsilon_2}\right)}, \qquad \text{(DR2)}$$

where indices 1 and 2 denote the flow and the substrate, respectively, U is the velocity, γ is the wavelength of the instabilities, and ε is the particle volume fraction. With U_2=0, γ=10-15 mm, and ($\varepsilon_2/\varepsilon_1$)-($\varepsilon_1/\varepsilon_2$)<1 (the flow is less concentrated then the substrate), instabilities can arise if the flow velocity U_1>0.12-0.15 m/s, which is the case in all our experiments.

Farin, M., Mangeney, A., and Roche, O., 2013, Dynamics, deposit and erosion processes in granular collapse over sloping beds: Journal of Geophysical Research, under revision.

Rowley, P.J., Kokelaar, P., Menzies, M., and Waltham, D., 2011, Shear-derived mixing in dense granular flows: Journal of Sedimentary Research, v. 81, p. 874-884.

SUPPLEMENTARY MOVIES DR1-5

Supplementary Movie DR1. Flow propagation on a granular substrate. General view of an initially fluidized flow of fine glass beads (d=80 µm, U=3.06 m s^{-1}) propagating on a rough substrate of steel beads (d=1590 µm). Movie speed is 40 times less than actual speed.

Supplementary Movie DR2. Flow propagation on a granular substrate. Close view of an initially fluidized flow of fine glass beads (d=80 µm, U=2.60 m s^{-1}) propagating on a smooth substrate of glass beads (d=80 µm). Movie speed is 40 times less than actual speed.

Supplementary Movie DR3. Flow propagation on a granular substrate. Close view of an initially fluidized flow of fine glass beads (d=80 µm, U=2.55 m s^{-1}) propagating on a rough substrate of steel beads (d=1590 µm). Movie speed is 40 times less than actual speed.

Supplementary Movie DR4. Flow propagation on a bidisperse granular substrate. Close view of an initially fluidized flow of fine glass beads (d=80 µm, U=2.67 m s^{-1}) propagating on a substrate of binary mixture of coarse steel beads (d=1590 µm) with fine glass beads (d=80 µm, black). The fines fill the network of coarse beads up to its height. The entrainment process is the same as in the case of a smooth substrate of fines only. Movie speed is 40 times less than actual speed.

Supplementary Movie DR5. Flow propagation on a bidisperse granular substrate. Close view of an initially fluidized flow of fine glass beads (d=80 µm, U=2.85 m s^{-1}) propagating on a substrate of binary mixture of coarse steel beads (d=1590 µm) with fine glass beads (d=80 µm, black). The fines fill the network of coarse beads only up to ~1-2 bead diameter from the top. The entrainment process is the same as in the case of a rough substrate of coarse particles only, though percolation of the fine flow particles is limited. Movie speed is 40 times less than actual speed.